

# AM1 Study of the Ground and Excited State Potential Energy Surfaces of Symmetric Carbocyanines

Javier Rodríguez,<sup>†</sup> Damián Scherlis,<sup>†</sup> Darío Estrin,<sup>\*,†</sup> Pedro F. Aramendía,<sup>‡</sup> and R. Martín Negri<sup>\*,‡</sup>

Laboratory of Thermodynamics and Laboratory of Photochemistry, INQUIMAE, Departamento de Química Inorgánica, Analítica y Química Física, Facultad de Ciencias Exactas y Naturales, Universidad de Buenos Aires, Pabellón II, Ciudad Universitaria, 1428 Buenos Aires, Argentina

Received: April 18, 1997; In Final Form: June 20, 1997<sup>⊗</sup>

Ground ( $S_0$ ) and first excited singlet state ( $S_1$ ) potential energy surfaces were calculated for a series of six symmetric carbocyanines as a function of the twisting angle ( $\theta$ ), around a carbon–carbon bond of the polymethine chain. The surfaces were computed using AM1 semiempirical quantum mechanical calculations. Rotations around different bonds were considered in order to determine the relevant rotation for isomerization, that is, the rotation with the lowest activation energy for the isolated molecule ( $E_0$ ). For that rotation, the computed values of  $E_0$  are in good agreement with values extrapolated from experiments in solutions of  $n$ -primary alcohols. The same holds for the computed transition energies between both surfaces for the thermodynamically stable N isomer ( $\theta = 0^\circ$ ) and the P photoisomer ( $\theta = 180^\circ$ ). The effects of chain length and pattern substitution of the indoline moiety on  $E_0$  were also analyzed for both surfaces. The shape of the potential surfaces referred as the Rullière's model holds in all cases for at least one rotational coordinate. The electrical dipole moment with respect to the center of electrical charges was calculated as a function of  $\theta$ . The calculations show that the dipole moment remains almost constant except in the vicinity of  $\theta = 90^\circ$ , where a sudden increase with a sharp peak was obtained in both surfaces. This gives a simple explanation for the well-known experimental observation that the activation energy on the excited state surface is independent of solvent polarity, as the angle of the transition state is smaller than  $90^\circ$ . On the other hand, the transition state is at  $\theta = 90^\circ$  on the ground state, and a polarity influence is predicted. An improvement in the description of the experimental isomerization rate constants in  $S_0$  is obtained for the two smallest carbocyanines considered when polarity contributions are included.

## Introduction

Carbocyanines are polymethine dyes that have applications in photographic processes,<sup>1</sup> in laser technology,<sup>2,3</sup> and as fluorescent probes in microheterogeneous systems.<sup>4–6</sup> The fluorescence and electron transfer properties, important for these applications, compete with an isomerization by carbon–carbon bond rotation, which takes place from the first excited singlet state produced by visible excitation of the thermodynamically stable conformation (N). Upon relaxation to the ground state photoisomer (P), the process continues by a thermal isomerization back to N. These isomerization processes involve the rotation of a segmental part of the molecule on both the ground state ( $S_0$ ) and the first singlet excited state ( $S_1$ ) potential surfaces.<sup>7–34</sup> Many parameters of both isomerizations, such as activation energies or quantum yields, have been determined in homogeneous solutions using fluorescence spectroscopy,<sup>7–17</sup> flash photolysis,<sup>11–23</sup> or photothermal methods.<sup>24–29</sup>

The potential energy diagram of Figure 1 will be referred in the text as Rullière's model<sup>12</sup> without any consideration about the possible quantum mechanical models that can lead to this surface shape, and without ascribing any particular physical property to the potential curves except that they are associated to singlet states. This model is usually adopted to account for the photophysical behavior of carbocyanines.<sup>14,17,19,23,30</sup> The isomerization coordinate is the twisting angle,  $\theta$ . Rullière's model assumes that a maximum exists in  $S_0$  at  $\theta = 90^\circ$  (the

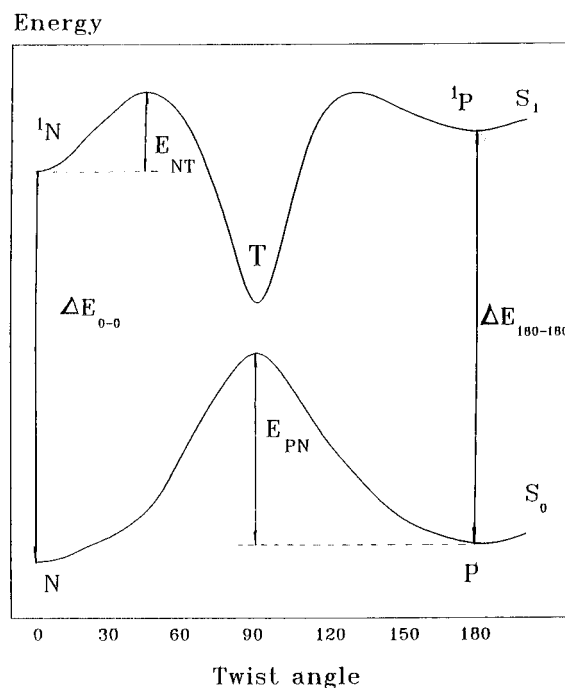


**Figure 1.** Scheme of the torsion angle dependence of the isomerization potential energy surfaces for the ground ( $S_0$ ) and excited ( $S_1$ ) states surfaces. This scheme is referred to in the text as the model of Rullière.<sup>12</sup>

perpendicular conformation), which corresponds to a minimum in  $S_1$ . This intermediate twisted state (T, see Figure 1) is obtained by rotation of a bond of the polymethine chain after

\* To whom correspondence should be addressed.

<sup>†</sup> Laboratory of Thermodynamics.

<sup>‡</sup> Laboratory of Photochemistry.

<sup>⊗</sup> Abstract published in *Advance ACS Abstracts*, August 1, 1997.

absorption of visible light. T decays to the ground state potential surface with a branching ratio for the possible isomeric ground state structures. P is referred as the "photoisomer", and  $^1P$  is its first excited singlet state. The model assumes that the isomerization coordinate  $\theta$  is the same for both surfaces.

The isomerization rate constants in solution are strongly dependent on the solvent. The Arrhenius activation energies,  $E_a$ , measured in a series of primary  $n$ -alcohols are dependent on solvent viscosity, due to the solvent friction on the rotation.<sup>9,10,17,31-33</sup> On the other hand, it has been found that for most of the symmetric carbocyanines,  $E_a$  is related to the viscosity activation energy of the solvent,  $E_\eta$ , by<sup>9,10,32,33</sup>

$$E_a = E_0 + aE_\eta \quad (1)$$

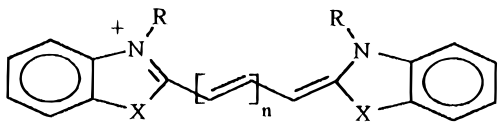
where  $E_0$  is the so-called intrinsic activation energy. The empirical parameter  $a$  accounts for the strength of the viscous effect.  $E_a$ ,  $E_0$ , and  $a$  are different in the ground and excited states. Different values of  $E_0$  and  $a$  can be obtained if different series of homologous solvents are used. There is experimental evidence of this fact for the cis-trans isomerization of diphenylbutadiene<sup>35</sup> and of a merocyanine (MC540).<sup>36</sup> However, it has been shown that for most of the symmetric carbocyanines  $E_0$  and  $a$  remain constant through the series on  $n$ -primary alcohols. In this case, according to eq 2 the only influence of the solvent on  $E_a$  is given by the solvent viscosity.<sup>6,9,10,14,17,31-33</sup>

In spite of the large amount of experimental studies, many aspects of the isomerization process are not well understood at present. (I) It is not possible to infer from those studies which is the relevant bond rotation, or if only one photoisomer is built up and if this situation changes for the different carbocyanines. Only for one carbocyanine was P identified by  $^1H$  NMR,<sup>37</sup> and evidences exist for other cases.<sup>37-39</sup> (II) It is also unclear why the activation energies do not depend on solvent polarity. During the rotation of a part of the molecule around one C-C bond of the polymethine chain, an important change of the dipole moment vector is expected, as a consequence of charge localization due to resonance breaking.<sup>8</sup> This should give, *a priori*, a contribution of solvent polarity to  $E_a$ . (III) Furthermore, this effect can cause rearrangement of other coordinates of the molecule and the solvent, which can make the isomerization a multicoordinate process.<sup>40</sup>

The aim of the present work is to explore these questions by using semiempirical AM1 quantum mechanical calculations. Potential energy surfaces for the ground and excited states were obtained as a function of the twist angle for a series of six symmetric carbocyanines, considered as isolated molecules. From these results,  $E_0$  and the transition energies between the ground and excited states of N and P were derived, and the values were compared to those deduced from experimental studies. Different twist angles were considered to determine the rotation of the lowest activation energy, *i.e.* the relevant rotation. Finally, the variation of the molecular dipole moment (referred to the center of electrical charge) along the isomerization coordinate was calculated in order to understand the role of solvent polarity on  $E_a$ .

The N configurations of the cyanines studied are shown in Table 1. The activation energy for the photoisomerization is the activation energy for the process  $^1N \rightarrow T$  on  $S_0$  and is indicated as  $E_{NT}$  in Figure 1. The thermal back-isomerization of P to N has an activation energy indicated by  $E_{PN}$ . Solvent effects were not considered in the calculations, so the calculated values of  $E_{NT}$  and  $E_{PN}$  must be compared to the intrinsic activation energy,  $E_0$  of eq 1. The transition energies  $\Delta E_{0-0}$  and  $\Delta E_{180-180}$  are the energies for the transitions  $N \rightarrow ^1N$  and  $P \rightarrow ^1P$ , respectively.

TABLE 1: Molecular Structure of the Normal Form (N) of Symmetric Carbocyanines



cyanine	$n$	X	R
DOCI	1	O	C <sub>2</sub> H <sub>5</sub>
DODCI	2	O	C <sub>2</sub> H <sub>5</sub>
DOTCI	3	O	C <sub>2</sub> H <sub>5</sub>
DTCI	1	S	C <sub>2</sub> H <sub>5</sub>
DTDCI	2	S	C <sub>2</sub> H <sub>5</sub>
HIDCI	2	C(CH <sub>3</sub> ) <sub>2</sub>	CH <sub>3</sub>

In addition to the AM1 calculations, experimental flash photolysis results<sup>17</sup> were reanalyzed to include a dielectric contribution to  $k_{PN}$  in order to check the role of solvent polarity.

### Experimental Section

**AM1 Calculations.** The isomerization potential energy surfaces  $S_0$  and  $S_1$  were computed using the semiempirical MOPAC package (Version 6.03) on an IBM Power-PC 7020. The AM1 parametrization was used.<sup>41,42</sup> This parametrization is known to be accurate for polar organic molecules.

The series of carbocyanine cations, 3,3'-diethyl oxacarbocyanine (DOCI), 3,3'-diethyl thiocarbocyanine (DTCI), 3,3'-diethyl oxadiazocarbocyanine (DODCI), 3,3'-diethyl thiadiazocarbocyanine (DTDCI), 3,3'-diethyl oxatricarbocyanine (DOTCI), and 1,1',3,3',3'-hexamethyl indodicarbocyanine (HIDCI) studied in this work are shown in Table 1. A full geometry optimization for the ground state of the N isomer cation was performed by using a restricted Hartree-Fock (RHF) closed shell algorithm. No influence of the counterion was considered on the calculations.

The ground state isomerization surface was constructed by performing a stepwise rotation around a chosen C-C bond of the polymethine chain, starting at the N geometry and fully optimizing all other geometrical parameters. The excited state isomerization surfaces were constructed by performing a configuration interaction (CI) calculation with 100 microstates at the ground state optimized geometries. These many states were used in order to achieve convergence of the CI energy with respect to the number of microstates within 1.0 kcal/mol and are believed to provide a fair approximation of correlation effects.

In addition to the evaluation of the isomerization surfaces, we calculated the dependence of the electrical dipole moment with the torsion angle for  $S_0$  and  $S_1$ . The electrical dipole moment was referred to the charge center of the molecule.

**Flash Photolysis.** The rate constants  $k_{PN}$  for DOCI and DTDCI in the series of primary alcohols from methanol to octanol have been previously reported.<sup>17</sup> In the present work, the values obtained in decanol were included and the whole set of rate constants simultaneously analyzed. The values of  $k_{PN}$  from ref 17 were measured by conventional flash photolysis with absorption detection.<sup>43</sup> In this work  $k_{PN}$  was measured by laser flash photolysis for DTDCI in ethanol and octanol at different temperatures using the second harmonic of a Nd:YAG laser (532 nm) as excitation source in a setup that was described elsewhere.<sup>44</sup>

### Results and Discussion

**AM1 Calculations of Potential Energy Surfaces.** Isomerization surfaces were constructed as a function of the torsion

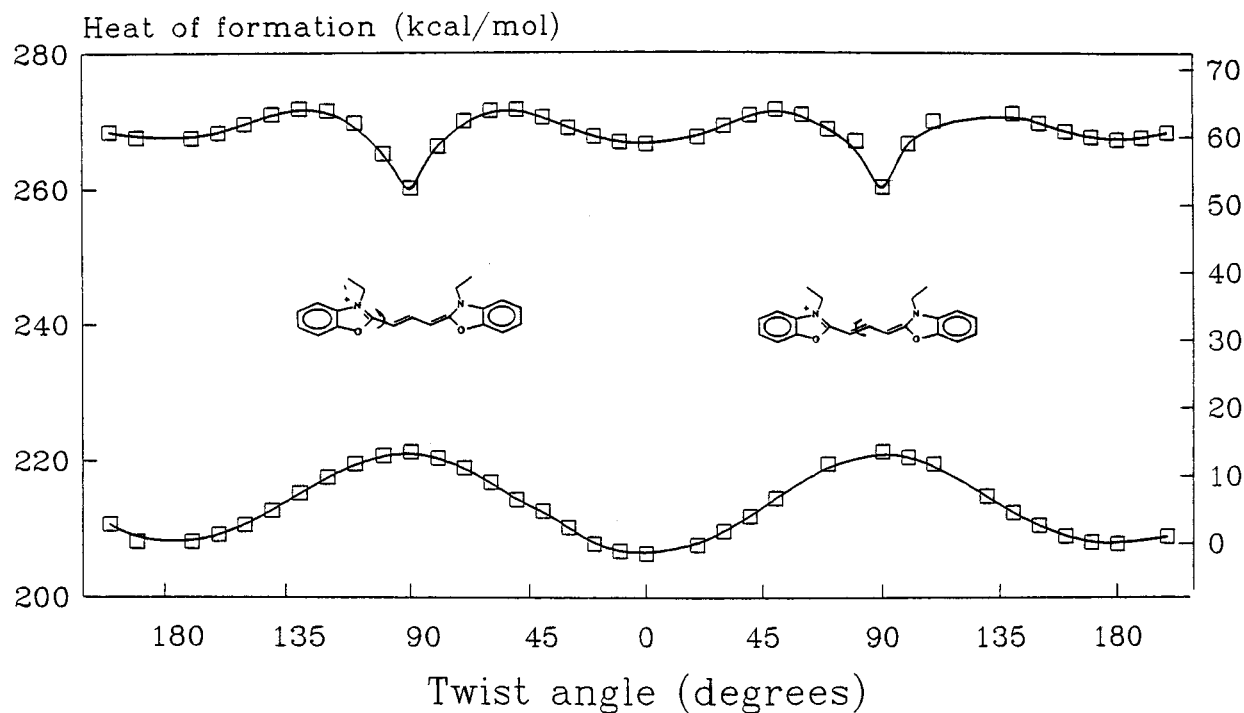


**Figure 2.** Computed isomerization potential energy surfaces for the  $S_0$  and  $S_1$  surfaces of DOCI. Rotations around two polyene bonds are shown, each beginning from the N conformation located at  $0^\circ$  in the center of the diagram. Open squares are the values of the actual calculations. The lines are smooth curves interpolated between the points. The right ordinate has its origin in the N ground state conformation.

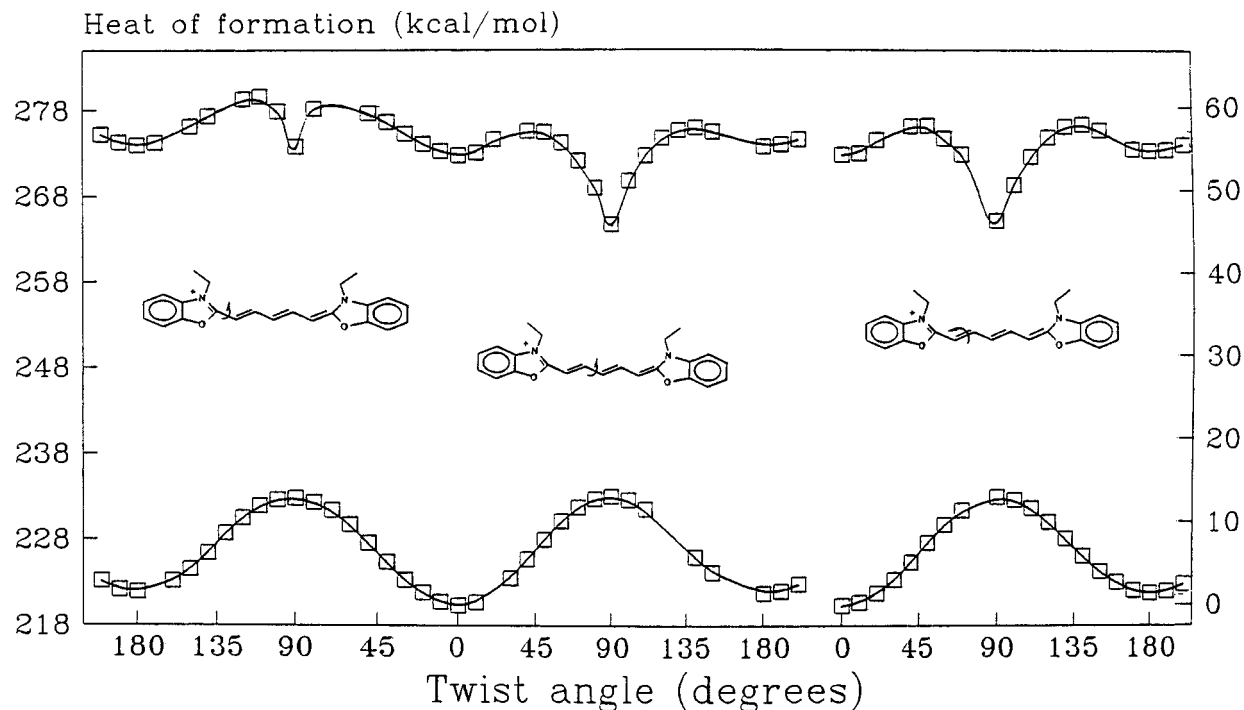


**Figure 3.** Computed isomerization potential energy surfaces for the  $S_0$  and  $S_1$  surfaces of DODCI. Same remarks as for Figure 2. In this case rotations around the three C–C bonds are shown. The right ordinate has its origin in the N ground state conformation.

angle by rotating different C–C bonds of the polymethine chain, one at a time. As illustrative examples, the surfaces for DOCI (torsion around the two different C–C polymethine bonds), DODCI (torsion around the three different bonds), and DOTCI (torsion around three different bonds) are presented in Figures 2, 3, and 4, respectively.

For DOCI, the rotation around the different bonds yield very similar potential energy surfaces and activation energies, in agreement with the qualitative Rullière's model. The result holds for  $S_0$  and  $S_1$ .

In the case of DODCI, rotation around any of the two bonds located within C–C atoms of the polyene chain yields the same activation energy. However, for the rotation around the bond connecting the polymethine chain to the end oxaindoline moiety a higher maximum is observed for the  $S_1$  surface (see Figure 3). This has already been pointed out by Awad et al.<sup>22</sup> Since the barrier for isomerization around this coordinate is much larger than the others, it is not likely that this path contributes to the experimental distribution of isomers. In this case two photoisomers are expected to be obtained at most upon

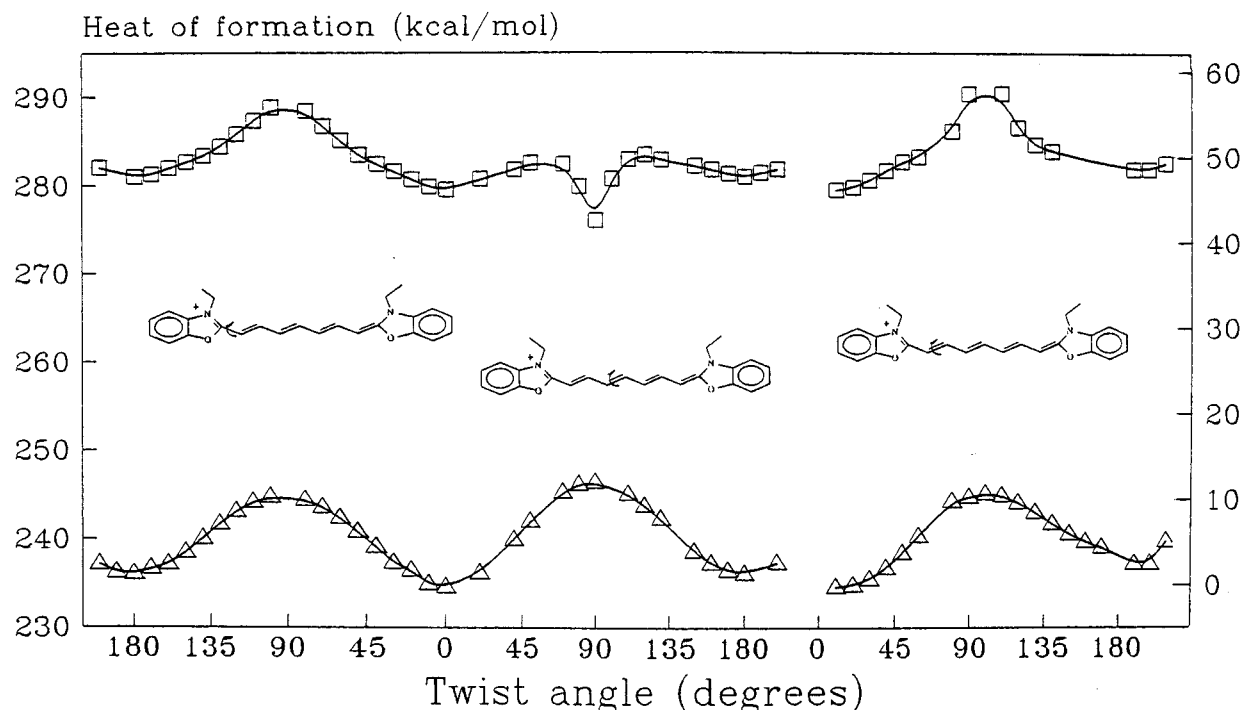


**Figure 4.** Computed isomerization potential energy surfaces for the  $S_0$  and  $S_1$  surfaces of DOTCI. Same remarks as for Figure 2. In this case rotations around three C–C bonds are shown. The right ordinate has its origin in the N ground state conformation.

excitation with visible light. The same shape and activation energies were obtained for the three rotations on the ground state. Similar results for both surfaces were obtained for the thia related compound, DTDCI.

In the case of DOTCI, the three torsional surfaces for the ground state were also very similar. On the other hand, on  $S_1$  a maximum was obtained at the perpendicular conformation, instead of the usual minimum, for two torsional angles. However, this fact does not affect the interpretation of DOTCI photoisomerization behavior in terms of the Rullière's model, since for the third torsional surface the usual  $90^\circ$  minimum and the lowest activation energy were obtained.

For all the cyanines considered at least one rotation yielded potential energy surfaces consistent with the Rullière's model.

From the above discussion, the possibility of different isomers coexisting cannot be ruled out. Each isomer is associated to the rotation of a different C–C bond with similar activation energies. The experimentally observed single-exponential behavior for an isomer's decay in all cases points to the existence of a single isomer or of two different types of isomers that behave kinetically in the same way. This last picture seems to be consistent with the calculations, as activation energies in  $S_0$  and  $S_1$  surfaces are identical for two coordinates. Nevertheless, it must be recalled that a 1 kcal/mol error in the surface energies can yield a factor of 5 in the ratio between rate constants, when applied to activation energies at room temperature (*i.e.*, if 1 kcal/mol is the difference in activation energies for two different twisting angles, the isomer with the smaller activation energy is formed in more than 80% yield). This is relevant since our semiempirical calculations are not expected to yield quantitative answers.

The lowest activation energies, calculated among the rotations of different bonds, are indicated by  $E_{PN}$  and  $E_{NT}$  in Table 2. These values can be associated to the parameter  $E_0$  in eq 1. The calculated  $E_{PN}$  and  $E_{NT}$  can be compared with previously reported values, referred to as  $E_{PN}^{exp}$  and  $E_{NT}^{exp}$ , which were obtained from experimental work. It is important to remark that  $E_{PN}^{exp}$  and  $E_{NT}^{exp}$  were not directly measured in gas phase, but

**TABLE 2: Activation Energies for the Thermal Back-Isomerization on the Ground State ( $E_{PN}$ ) and for the Photoisomerization on the First Singlet Excited State ( $E_{NT}$ )**

	DOCI	DODCI	DOTCI	DTCI	DTDCI	HIDCI
	$E_{PN}$ (kJ/mol)					
experimental <sup>a</sup>	61 <sup>b</sup>	57 <sup>d</sup>	43	60 <sup>b</sup>	47	47
	$E_{NT}$ (kJ/mol)					
calculated	54	45	41	50	40	45
experimental <sup>a</sup>	10	11 <sup>d</sup>	20	10	24	20
calculated	19	11	12	4	5	21

<sup>a</sup> Values referred to as  $E_{PN}^{exp}$  and  $E_{NT}^{exp}$  in the text, taken from ref 17, except as indicated. <sup>b</sup> Values recovered using eq 2, but without considering the data in decanol. <sup>c</sup> Recovered values when the data for all solvents, including decanol, are fitted by eq 3. <sup>d</sup> From ref 20.

extrapolated from experimental data obtained in solution, as is described in the literature.<sup>17</sup> The values of  $E_{PN}^{exp}$  and  $E_{NT}^{exp}$  are also shown in Table 2.

For the ground state surface the overall agreement between  $E_{PN}$  and  $E_{PN}^{exp}$  is very good. The calculated  $E_{PN}$ , and the "experimental" values as well, decreases with the polymethine chain length. This can be explained in terms of a valence bond picture, since in cyanines with longer polymethine chains the resonance delocalization energy in the fragments at the perpendicular conformation is more important.

The calculation is able to predict that the activation energies are systematically larger on  $S_0$  than on  $S_1$ :  $E_{PN} > E_{NT}$ . This is also in agreement with the results from experiments. The agreement between  $E_{NT}$  and  $E_{NT}^{exp}$  is excellent for DODCI and HIDCI (see Table 2), but the difference is 50% for DOCI and more than 200% for DTCI and DTDCI. This is probably due to the fact that the semiempirical calculations rely on parametrizations derived from ground state experimental data, which include correlation effects. In that sense these effects are not considered in a consistent way by performing CI calculations; thus, the estimation of properties in the excited states involve a larger uncertainty than in the ground state. The difference between  $E_{NT}$  and  $E_{NT}^{exp}$  is larger for the thiocarbocyanines than

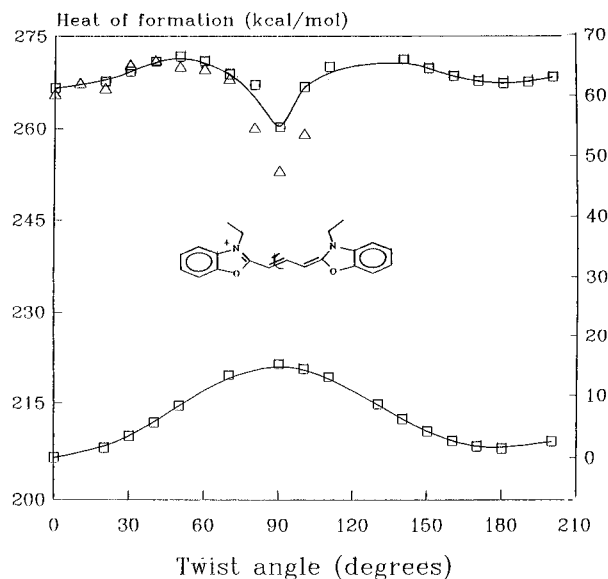


**Figure 5.**  $S_0$  and  $S_1$  surfaces of DOCI, for the relevant rotation, showing the effect of optimizing the  $S_1$  geometry considering full relaxation of the geometrical parameters: ( $\square$ ) calculated using  $S_0$  relaxed geometry; ( $\triangle$ ) calculated using  $S_1$  fully relaxed geometry.

for the oxo compounds. This could be related to a poorer performance of semiempirical methods in compounds containing elements of the third period.<sup>45</sup>

Another possible source of errors in  $E_{NT}$  could be that the excited state calculations are based on a ground state optimized geometry. However, we checked the validity of this approximation by computing the isomerization potential energy surface for DOCI, fully optimizing the excited state geometry step by step *i.e.*, allowing all other coordinates to achieve their minimum energy after a rotation step of the torsion angle selected. In this way, a relaxed geometry is obtained with respect to other coordinates. We observed that relaxation only affects appreciably the energies at torsional angles close to  $90^\circ$ , implying that this approximation affects only very slightly the computed activation energies. The energy decrease at the T state using the fully relaxed geometry is more in agreement with the physical picture of Figure 1. In that figure, the difference of energy between the surfaces  $S_0$  and  $S_1$  at  $90^\circ$  was set to a very small value in order to account for the very short lifetime of the T state.<sup>22</sup> However, even considering geometry relaxation in the  $S_1$  surface the energy gap at  $\theta = 90^\circ$  is still large, as shown in Figure 5. On the other hand, Rullière's model with a small energy difference seems to account very well for the experimental results in solution. This subject has been extensively discussed by Momicchioli and co-workers.<sup>8</sup> Then, the reduction of the energy gap may be ascribed to solvent effects. Simple dielectric solvation arguments, based on dipole moment interactions, do not provide a reasonable answer in this case, since in both ground and excited states the dipole moments are large and comparable at the T conformation. More sophisticated models of solvation are probably necessary to account for this effect<sup>46–48</sup> as discussed below.

The fact that coordinate relaxation affects the energy of  $S_1$  at torsion angles greater than the value at the maximum (transition state) supports the description of the isomerization as a one-coordinate process.

We have also evaluated the transition energies  $N \rightarrow {}^1N$  and  $P \rightarrow {}^1P$ , which are the energy differences between the  $S_0$  and  $S_1$  surfaces evaluated at 0 and 180 degrees. The results, together with the available experimental information,<sup>27,38,49</sup> are presented in Table 3. The agreement with the experimental results is

**TABLE 3: Transition Energies (in nm) between  $S_0$  and  $S_1$  for the N Configuration ( $\Delta E_{0-0}$ ) and the P Photoisomer ( $\Delta E_{180-180}$ )**

	DOCI	DODCI	DOTCI	DTCI	DTDCI	HIDCI
	$\Delta E_{0-0}$ (nm)					
experimental <sup>a</sup>	490	560	696	564	665	647
calculated	471	529	650	556	676	650
	$\Delta E_{180-180}$ (nm)					
experimental	490 <sup>b</sup>			545 <sup>b</sup>	650 <sup>c</sup>	
calculated	482	534	650	546	684	643

<sup>a</sup> In ethanol, from ref 49. <sup>b</sup> From ref 38. <sup>c</sup> From ref 27.

**TABLE 4: Net Charges in Fragments Obtained upon Rotation of the Polymethine Chain for DOCI, DODCI, and DOTCI**

DOCI						
twist angle	0°		90°		180°	
	$Q_A$	$Q_B$	$Q_A$	$Q_B$	$Q_A$	$Q_B$
$S_0$	0.355	0.645	0.067	0.933	0.343	0.657
$S_1$	0.487	0.513	0.812	0.188	0.459	0.540
DODCI						
twist angle	0°		90°		180°	
	$Q_A$	$Q_B$	$Q_A$	$Q_B$	$Q_A$	$Q_B$
$S_0$	0.576	0.424	0.895	0.105	0.580	0.420
$S_1$	0.476	0.524	0.120	0.879	0.487	0.513
DOTCI						
twist angle	0°		90°		180°	
	$Q_A$	$Q_B$	$Q_A$	$Q_B$	$Q_A$	$Q_B$
$S_0$	0.387	0.613	0.076	0.924	0.399	0.601
$S_1$	0.501	0.499	0.876	0.124	0.527	0.473

remarkable. The small Stokes shifts observed in alcohol solutions also confirm the fact mentioned above related to the small changes in geometry between N and  ${}^1N$ , and P and  ${}^1P$  for the symmetric carbocyanines.

Up to this point all the results presented were based on the assumption that the molecules are isolated. However, it is extremely important to understand how the systems will interact with their surroundings, in order to relate the computational results to the experiments in solution. The interaction with polar environments is linked to the solute charge distribution. It can be seen from the calculations that there is a significant charge redistribution upon rotation of a torsion angle. The net charges in the fragments obtained upon rotation of one selected bond of the polymethine chain for DOCI, DODCI, and DOTCI are given in Table 4 at the N, T, and P conformations. They are in agreement with values published for the compound bis-

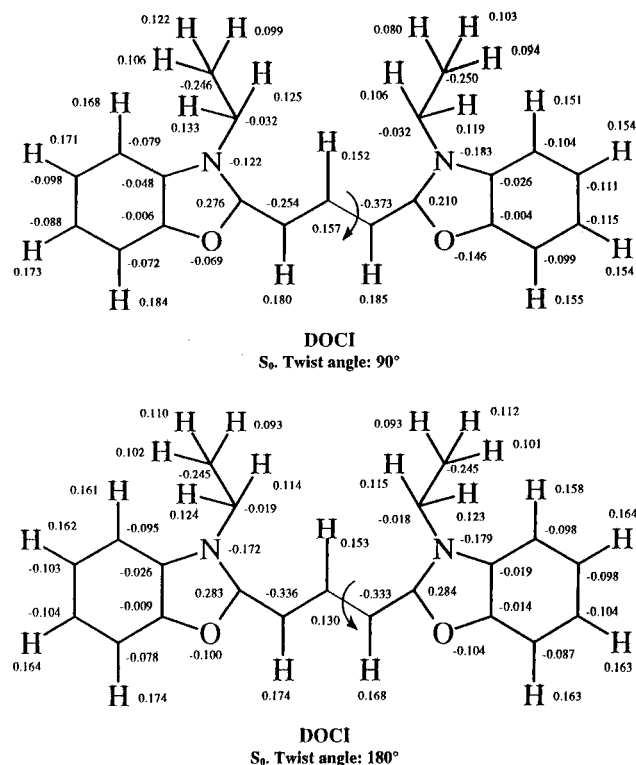


**Figure 6.** Mulliken charge distribution for DOCI in the N, T, and P conformations of  $S_0$ . N and P are plane structures. The T conformation is not planar and was calculated for rotation around the relevant rotation.

(phenylaminopenthamine) cyanine,<sup>50</sup> which can be related to DOCI and DTCl.

For  $S_0$  the net charges in the A and B fragments (left and right, respectively, in Table 4) can be rationalized in terms of a simple valence bond picture. Considering resonance structures involving the nitrogen and the polyenic carbon atoms, the positive charge can be localized more easily in fragment A in DODCI and in fragment B in DOCI and DOTCl. This is in agreement with the net charges reported in Table 4 for the N, T, and P conformations.

Remaining in  $S_0$ , for the T conformation, valence bond arguments predict that the structure with charge localization in one moiety and all atoms carrying a complete octet should be the most favorable.<sup>8,42</sup> This is in agreement with the net charges given in Table 4. The charge transfer nature of T is a quite general phenomenon that arises in the cis–trans isomerizations of bonds with a partial double-bond character, as long as the two halves have different abilities for attracting electrons, and is related to the effect of sudden polarization. This analysis has been applied by Michl and Bonacic-Koutecky to a great variety of reactions.<sup>51,52</sup> The fact that the T geometry does not have a biradicaloid character was also confirmed by performing CI calculations at that geometry, without observing any significant change in the computed energy.

In the  $S_1$  case there is also a significant charge localization upon rotation, but the charge tends to localize in fragment B in DODCI and in A in DOCI and DOTCl, respectively, contrarily to the  $S_0$  case. Valence bond arguments for a biradical state predict that structures with charge localization in those moieties are the most favorable at the T conformation.

Although these valence bond arguments are useful to explain the net charges presented in Table 4, it should be kept in mind that the charge distribution is more complex. For instance, there are significant positive charges also on H atoms, and N and C atoms hold negative charges. As an illustrative example, the Mulliken populations for DOCI are shown in Figure 6.

The dipole moment in charged systems is not translationally invariant, unless it is evaluated with the origin at the center of electric charge.<sup>53</sup> We have used the dipole moment computed in this way as an indicator of the charge distribution. The results obtained for the dipole moment as a function of the torsion angle for the  $S_0$  and  $S_1$  surfaces of DOCI and DODCI are presented in Figures 7 and 8, respectively. Previous AM1 calculations for the N and P isomers agree with our results.<sup>28</sup> In all cases the electrical dipole moment has a slight variation as a function of  $\theta$ , until a sharp peak appears in the neighborhood of  $\theta = 90^\circ$ . (The change is more abrupt for  $S_1$ .) Therefore, solvent polarity is predicted to have little or no influence on the activation energy on  $S_1$  because the transition state is located at  $\theta < 90^\circ$ , in the region where the change in dipole moment is very small.<sup>8</sup> The predicted low influence of solvent polarity for this case is in agreement with the experimental results obtained in *n*-primary alcohols for most of the symmetric carbocyanines, for which  $k_{NT}$  depends only on solvent viscosity and eq 2 holds for  $S_1$ . The opposite behavior is predicted for the P  $\rightarrow$  N isomerization on  $S_0$ , as the transition state is exactly at the perpendicular configuration.

**Polarity Effects on the Ground State Isomerization.** On  $S_0$  the transition state and the maximum in dipole moment coincide. Thus, an influence of polarity on  $k_{PN}$  is expected. This influence was not observed experimentally for DTDCI, DODCI, DOTCl, and HIDCl in the series of *n*-primary alcohols from methanol to decanol.<sup>10,17</sup> No influence of polarity was observed for the smallest cyanines, DOCI and DTCl, from methanol to octanol. For these cases, the observed values of  $k_{PN}$  were analyzed according to the empirical model

$$k_{PN} = \frac{D}{(\eta/\eta_0)^a} \exp\left(-\frac{E_0}{RT}\right) \quad (2)$$

where  $\eta$  is the viscosity of the solvent,  $\eta_0 = 1$  cP, and  $D$  and  $a$  are adjustable parameters. This model was originally developed by Fischer and co-workers for the case of *trans*-stilbene photoisomerization.<sup>54</sup> It was based on the free volume theory for viscosity and the assumption that the free volume required by the rotating group, the so-called activation volume, is a fraction ( $0 < a \leq 1$ ) of the solvent critical free volume for translational diffusion.<sup>55</sup> However, Bagchi and Oxtoby<sup>56</sup> showed that the  $\eta^{-a}$  dependence naturally arises when the frequency dependence of the friction exerted by the solvent at the barrier region is taken into account, without referring to an activation volume model. The parameter  $a$  is the same as introduced in eq 1, and the departure of its value from unity is an indication of frequency-dependent friction effects. For the case of DOCI and DTCl from methanol to octanol the reported values of  $\ln D$ ,  $a$ , and  $E_0$  fitted by eq 2 are  $\ln(D/\text{ms}^{-1}) = 21 \pm 1$ ,  $a = 0.30 \pm 0.03$ ,  $E_0 = 61 \pm 2$  kJ/mol for DOCI and  $\ln(D/\text{ms}^{-1}) = 22 \pm 1$ ,  $a = 0.17 \pm 0.04$ ,  $E_0 = 60 \pm 1$  kJ/mol for DTCl.

However, we have previously reported that eq 2 does not fit the rate constants of DOCI and DTCl when the data for decanol are included. For decanol the values of  $k_{PN}$  at a fixed temperature are higher than for octanol and pentanol and similar to the values in ethanol.<sup>17</sup> When the data for decanol are included, the quality of the fit is reduced and the recovered parameters are  $\ln(D/\text{ms}^{-1}) = 21 \pm 1$ ,  $a = 0.12 \pm 0.05$ ,  $E_0 = 65 \pm 3$  kJ/mol for DOCI and  $\ln(D/\text{ms}^{-1}) = 21.1 \pm 0.8$ ,  $a = 0.20 \pm 0.04$ ,  $E_0 = 57 \pm 2$  kJ/mol for DTCl.

Therefore, based on the predicted influence of solvent polarity, we consider a modification of the empirical model to take into account the effect of dielectric interactions on the activation energy

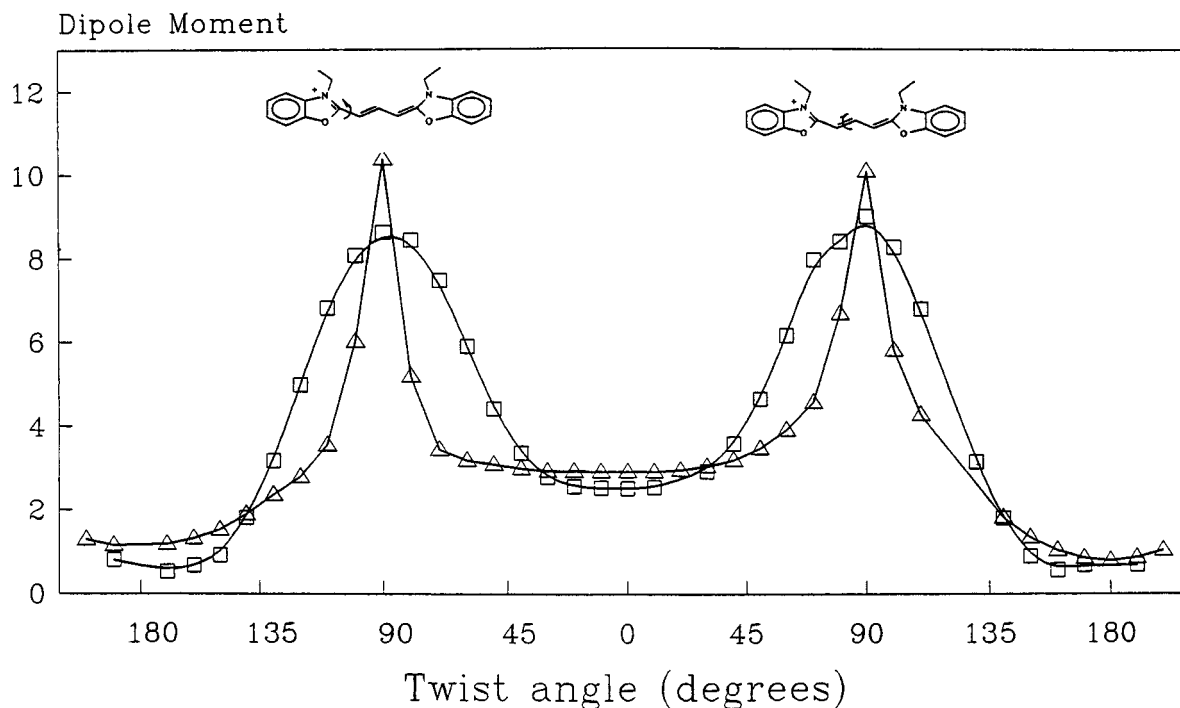


**Figure 7.** Dipole moment dependence on the torsion angle for DOCI in the  $S_0$  ( $\square$ ) and  $S_1$  ( $\triangle$ ) surfaces. Rotations about two polyene bonds are shown. Dipole moments are calculated with respect to the center of charges of the carbocyanine cation.

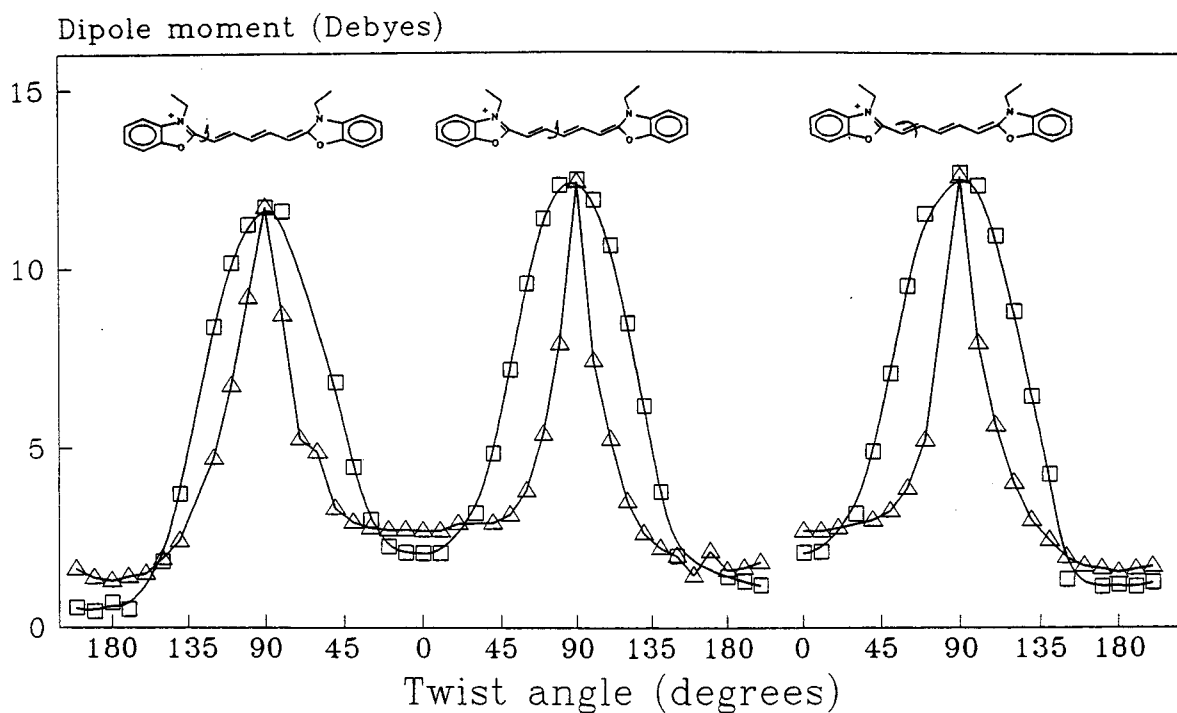


**Figure 8.** Dipole moment dependence on the torsion angle for DODCI in the  $S_0$  ( $\square$ ) and  $S_1$  ( $\triangle$ ) surfaces. Rotations about three polyene bonds are shown.

$$k_{\text{PN}} = \frac{D}{(\eta/\eta_0)^a} \exp\left(-\frac{E_0}{RT} - \frac{E_{\text{diel}}}{\epsilon^2 RT}\right) \quad (3)$$

where  $E_{\text{diel}}$  takes into account the interaction between the solvent dipole and the solute dipole. In this model the explicit dependence of solvent viscosity is kept the same as that in eq 2, but the polarity effects on the activation are considered by introducing an additional term to  $E_a$ . The  $\epsilon^{-2}$  dependence was recently proposed by Harju et al. to account for solute–solvent dipole–dipole interactions in the case of the polar molecule (dibenzylmethine)boron difluoride, which has a high dipole

moment at the transition state.<sup>47</sup> Although DOCI and DTICI are cationic molecules, we decided to use the  $\epsilon^{-2}$  dependence because they have also a high dipole moment in the transition state in  $S_0$ , as it was described in the previous section (see also Figures 7 and 8). On the other hand, it can be discussed whether the carbocyanine is in solution as an ion pair or as a dissociated cation. The ion pair motions are expected to be less influenced by solvent polarity and are certainly preferred in nonpolar solvents, whereas the dissociated cation is most likely in polar solvents such as methanol or ethanol, considering the dilute solutions normally used in photophysical studies (ca.  $10^{-6}$  M).

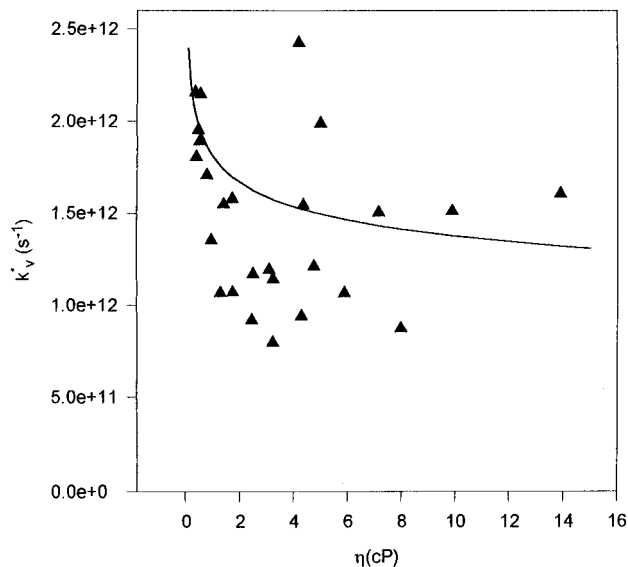


**Figure 9.** Reduced constant  $k_v^*$  (▲) and  $F(\eta) \equiv D/\eta^a$  (—) for DOCI as a function of  $\eta$ .  $D = 1.32 \times 10^{12} \text{ s}^{-1}$ ,  $a = 0.12$ ,  $E_0 = 65 \text{ kJ/mol}$ .

We are not considering the solute point charge solvent dipole interaction, assuming that the center of charge does not move or changes its position very little with respect to the center of mass of the molecule. This is a reasonable approximation. In this case the point charge dipole interaction provides only a constant background to the sharply changing dipole–dipole interactions. Nevertheless, it is not our aim to discuss the dependence of  $k_{PN}$  with solvent polarity on a rigorous theoretical basis, which is beyond the scope of this paper, but to show that a polarity correction is absolutely necessary to account for the experimental results, as is described in the next paragraphs of this section.

The fit according to eq 3 has a mean square deviation that is half the value of the corresponding to the fit to eq 2, when using the complete set of solvents. The fitted values of the parameters, calculated using eq 3 are  $\ln(D/\text{ms}^{-1}) = 15.7 \pm 1$ ,  $a = 0.52 \pm 0.06$ ,  $E_0 = 52 \pm 2 \text{ kJ/mol}$ ,  $E_{\text{diel}} = -159 \pm 20 \text{ kJ/mol}$  for DOCI and  $\ln(D/\text{ms}^{-1}) = 19.0 \pm 1$ ,  $a = 0.31 \pm 0.03$ ,  $E_0 = 51 \pm 3 \text{ kJ/mol}$ ,  $E_{\text{diel}} = -378 \pm 169 \text{ kJ/mol}$  for DTCl.

The standard deviation is significantly reduced when using eq 3, but this could be, in principle, only the effect of introducing an additional fitting parameter. Therefore, we use the reduced constants,  $k_{PN}^*$ , in order to better compare the quality of both fits. The reduced constants are defined in a different way, depending on which model is considered

$$k_v^* = k_{PN} \exp\left(\frac{E_0}{RT}\right) \quad (4)$$

when only viscous effects are considered and

$$k_{v,d}^* = k_{PN} \exp\left(\frac{E_0}{RT} + \frac{E_{\text{diel}}}{\epsilon^2 RT}\right) \quad (5)$$

when viscous and dielectric interactions are taken into account. In eqs 4 and 5  $k_{PN}$  is the experimental rate constant.

If the fits were of good quality, then in both cases  $k_v^*$  or  $k_{v,d}^*$  should have a hyperbolic dependence on  $\eta$ , given by  $D/\eta^a$ . For each cyanine, the values of  $E_0$ ,  $D$ , and  $a$  are those listed above, which are different for each model. For the case of DOCI,  $k_v^*$  and  $F(\eta) \equiv D/\eta^a$  are simultaneously represented as a function of  $\eta$  in Figure 9, and in Figure 10,  $k_{v,d}^*$  and  $D/\eta^a$  are plotted. Clearly  $k_{v,d}^*$  is almost coincident with  $D/\eta^a$ , but  $k_v^*$  is far from being coincident. A similar behavior was obtained for DTCl,

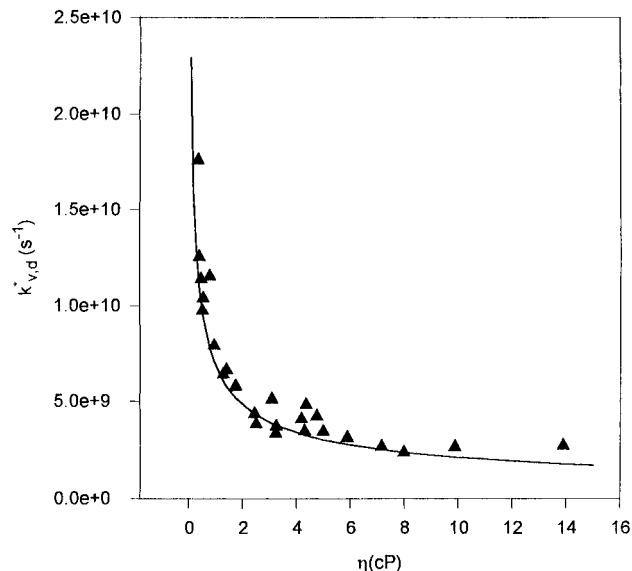


**Figure 10.** Reduced constant  $k_{v,d}^*$  (▲) and  $F(\eta) \equiv D/\eta^a$  (—) for DOCI as a function of  $\eta$ .  $D = 6.92 \times 10^9 \text{ s}^{-1}$ ,  $a = 0.52$ ,  $E_0 = 52 \text{ kJ/mol}$ ,  $E_{\text{diel}} = -159 \text{ kJ/mol}$ .

although with a larger dispersion than for DOCI in both fits. When the electric interactions are considered, the agreement of the experimental  $E_0$  values with the computed ones is excellent (Table 2). For the other carbocyanines very little polarity effect is observed.

The magnitude of the polarity effects increases from methanol to decanol, that is with decreasing solvent polarity, due to the  $\epsilon^{-2}$  dependence of the correction term and the negative sign of  $E_{\text{diel}}$ . Although the model is very crude, in particular because of the reasons discussed later in this section, the results obtained using that model show the necessity to consider not only the viscous interaction but also the polarity effects.

The experimental results presented in this paper were obtained in a series of analogous solvents, that is in the series of *n*-primary alcohols. This is indispensable in order to keep constant the possible influence of specific solute–solvent effects on  $E_0$  and  $a$ . For example, values of  $E_0$  as different as 0.7 and 4.7 kcal/mol in alcohols and alkanes were reported by Keery and Fleming<sup>35</sup> for the isomerization of diphenylbutadiene. Onganer et al.<sup>36</sup> have reported also different values of  $E_0$  and  $a$  for the cis–trans isomerization of merocyanine 540 in *n*-alcohols and *n*-alkanenitriles (i.e.,  $a = 0.623$  and  $0.883$ , respectively). Reference 8 reports the experimental activation energy  $E_a$  for the P → N thermal isomerization of DTCl and DOCI in only three solvents, which have very different chemical structures and properties (methanol, dichloromethane, and chlorobenzene). The nonsystematic analysis of the solvent polarity influence described by the authors, who do not report any quantitative reference to viscosity effects, i.e.  $E_0$  or  $a$  values, and only consider the influence of static (equilibrium) solvation effects, cannot be generalized and can hardly be applied to the series of *n*-alcohols. Moreover, they observe an increase in activation energy with decreasing dielectric constant, while we observe that the isomerization rates are faster in decanol than in ethanol. This result cannot be accounted for by static dipole solvation arguments.

Photoisomerization is a dynamic process and both static and dynamic solvent effects must be taken into account, which may operate in opposite directions. The electrical interaction between carbocyanines and the dipolar solvent involves static interactions derived from charge distributions and dynamic effects due to the fast changing dipole moment. The static or equilibrium



effects cause an increase of isomerization rates (or decrease of activation energies) with solvent polarity, since the polar transition state is stabilized in polar solvents, while dynamic effects cause a retardation in isomerization rates. Positive and negative values for  $E_{\text{diel}}$  in eq 3 are related to dominant static and dynamic effects, respectively. For the isomerization of the compound (dibenzylmethine)boron difluoride, Harju et al.<sup>47</sup> find an equilibrium situation in the series of *n*-nitriles but a nonequilibrium solvation in the more associated *n*-alcohols, which have slower relaxation times.

The dynamic interactions introduce a dielectric friction proportional to the Debye relaxation time of the solvent, which increases with the aliphatic chain length. For example, dielectric friction influences the rotational correlation times of DOCI, DTCl,<sup>57</sup> and the related compound merocyanine 540<sup>36</sup> but does not influence the rotation of the other carbocyanines.<sup>57</sup> This additional friction contributes to reduce  $k_{\text{PN}}$  from methanol to decanol, contrary to the static effect. Both effects might compensate partially to mask the polarity influence on ground state isomerization. For this reason, and taking into account that the effect of polarity is not the main one in the isomerization dynamics and that the complete mathematical treatment is rather cumbersome, it is not possible at present to discriminate how dynamic and static effects contribute to  $k_{\text{PN}}$  for the symmetric carbocyanines. Further experimental results, for example considering other series of homologous solvents, are needed.

**Acknowledgment.** P.F.A., D.E., and R.M.N. are members of the Carrera del Investigador Científico (Research Staff) of Consejo Nacional de Investigaciones Científicas y Técnicas (CONICET, Argentina). Research was supported by grants from UBA (EX-025 and EX-J002) and Fundación Antorchas (Argentina). J.R. is a student fellow of GTZ (Germany) and INQUIMAE.

## References and Notes

- (1) (a) Sturmer, D. M. *Synthesis and properties of cyanine and related dyes. Special topics in heterocyclic chemistry*; Weissberger, A., Taylor, E. C., Eds.; John Wiley & Sons: New York, 1977. (b) Sturmer, D. M.; Heseltine, D. W. *The theory of the photographic process*, fourth ed.; James, T. H., Ed.; Macmillan Publishing Co: New York, 1977; Chapter 8.
- (2) Mialocq, J. C.; Goujon, P.; Arvis, M. *J. Chim. Phys.* **1979**, *76*, 1067.
- (3) Arthurs, E. G.; Bradley, D. J.; Roddie, A. G. *Appl. Phys. Lett.* **1972**, *20*, 125.
- (4) Waggoner, A. *J. Membr. Biol.* **1976**, *27*, 317.
- (5) Waggoner, A. S.; Grinvald, A. *Ann. N.Y. Acad. Sci.* **1977**, *303*, 217.
- (6) Grieser, F.; Lay, M.; Thistlethwaite, P. J. *J. Phys. Chem.* **1985**, *89*, 2065.
- (7) Van der Auweraer, M.; Van den Zegel, M.; Boens, N.; De Schryver, F. C.; Willig, F. *J. Phys. Chem.* **1986**, *90*, 1169.
- (8) Ponterini, G.; Momicchioli, F. *Chem. Phys.* **1991**, *151*, 111.
- (9) Korppi-Tommola, J. E. I.; Hakkarainen, A.; Hukka, T.; Subbi, J. *J. Phys. Chem.* **1991**, *95*, 8482.
- (10) Ponterini, G.; Caselli, M. *Ber. Bunsen-Ges. Phys. Chem.* **1992**, *96*, 564.
- (11) Dempster, D. N.; Morrow, T.; Rankin, R.; Thompson, G. F. *J. Chem. Soc. Faraday Trans. 2* **1972**, *68*, 1479.
- (12) Rullière, C. *Chem. Phys. Lett.* **1976**, *43*, 303.
- (13) Jaradías, J. *J. Photochem.* **1980**, *13*, 35.
- (14) Velsko, S. P.; Fleming, G. R. *Chem. Phys.* **1982**, *65*, 59.
- (15) Berndt, K.; Dürr, H.; Feller, K. H. *Z. Phys. Chem. Leipzig* **1987**, *268*, 250.
- (16) Krieg, M.; Redmond, R. W. *Photochem. Photobiol.* **1993**, *57*, 472.
- (17) Aramendía, P. F.; Negri, R. M.; San Román, E. *J. Phys. Chem.* **1994**, *98*, 3165.
- (18) Magde, D.; Windsor, M. W. *Chem. Phys. Lett.* **1974**, *27*, 31.
- (19) Sundström, V.; Gillbro, T. *J. Phys. Chem.* **1982**, *86*, 1788.
- (20) Velsko, S. P.; Waldeck, D. H.; Fleming, G. R. *J. Chem. Phys.* **1983**, *78*, 249.
- (21) Kasatani, K.; Kawaski, M.; Sato, H. *J. Phys. Chem.* **1984**, *88*, 5451.
- (22) Awad, M. M.; McCarthy, P. K.; Blanchard, G. J. *J. Phys. Chem.* **1994**, *98*, 1454.
- (23) Chibisov, A. K.; Zakharova, G. V.; Görner, H.; Sogulyaev, Y. A.; Mushkalo, I. L.; Tolmachev, A. I. *J. Phys. Chem.* **1995**, *99*, 886.
- (24) Bilmes, G. M.; Tocho, J. O.; Braslavsky, S. E. *Chem. Phys. Lett.* **1987**, *134*, 335.
- (25) Scaffardi, L.; Bilmes, G. M.; Schinca, D.; Tocho, J. O. *Chem. Phys. Lett.* **1987**, *140*, 163.
- (26) Bilmes, G. M.; Tocho, J. O.; Braslavsky, S. E. *J. Phys. Chem.* **1988**, *92*, 5985.
- (27) Bilmes, G. M.; Tocho, J. O.; Braslavsky, S. E. *J. Phys. Chem.* **1989**, *93*, 6696.
- (28) Churio, M. S.; Angermund, K. P.; Braslavsky, S. E. *J. Phys. Chem.* **1994**, *98*, 1776.
- (29) Zhu, X. R.; Harris, J. M. *Chem. Phys.* **1990**, *142*, 301.
- (30) Bäuml, W.; Penzkofer, A. *Chem. Phys.* **1990**, *140*, 75.
- (31) Laitinen, E.; Ruuskanen-Järvinen, P.; Rempel, U.; Helenius, V.; Korppi-Tommola, J. E. I. *Chem. Phys. Lett.* **1994**, *218*, 73.
- (32) Hara, K.; Akimoto, S. *J. Phys. Chem.* **1991**, *95*, 5811.
- (33) Fleming, G. R.; Waldeck, D. H.; Keery, K. M.; Velsko, S. P. *Nato ASI Ser., Ser. C* **1984**, *127*, 67.
- (34) Murphy, B.; Sauerwein, H.; Drickamer, G.; Schuster, G. B. *J. Phys. Chem.* **1994**, *98*, 13476.
- (35) Keery, K. M.; Fleming, G. R. *Chem. Phys. Lett.* **1982**, *93*, 322.
- (36) Onganer, Y.; Yin, M.; Bessire, D. R.; Quitevis, E. L. *J. Phys. Chem.* **1993**, *97*, 2344.
- (37) Ghelli, S.; Ponterini, G. *J. Mol. Structure* **1995**, *355*, 193.
- (38) Baraldi, I.; Carnevali, A.; Momicchioli, F.; Ponterini, G. *Spectrochim. Acta* **1993**, *49A*, 471.
- (39) Kolesnikov, A. M.; Mikhailenko, F. A. *Usp. Khim.* **1987**, *56*, 466; *Russ. Chem. Rev.* **1987**, *56*, 275.
- (40) Zhu, S. B.; Robinson, G. W. *Chem. Phys. Lett.* **1988**, *153*, 539.
- (41) Dewar, M. J. S.; Zebisch, E. G.; Healy, E. F.; Stewart, J. J. P. *J. Am. Chem. Soc.* **1985**, *107*, 3902.
- (42) Hirst, D. M. *A Computational Approach to Quantum Chemistry*; Blackwell Scientific Publications: Oxford, 1990.
- (43) González, M. C.; San Román, E. *J. Phys. Chem.* **1989**, *93*, 3536.
- (44) Dariao, M. E.; Völker, A.; Aramendía, P. F.; San Román, E. *Langmuir* **1996**, *12*, 2932.
- (45) Dewar, M. J. S.; Reynolds, C. H. *J. Comput. Chem.* **1986**, *7*, 140.
- (46) Nee, T. W.; Zwanzig, F. J. *J. Chem. Phys.* **1970**, *52*, 6353.
- (47) Harju, T. O.; Korppi-Tommola, J. E. I.; Huizer, A. H.; Harmo, C. A. G. O. *J. Phys. Chem.* **1996**, *100*, 3592.
- (48) Reynolds, L.; Gardechi, J. A.; Frankland, S. J. V.; Horng, M. L.; Maroncelli, M. *J. Phys. Chem.* **1996**, *100*, 10337.
- (49) Negri, R. M. Ph.D. Thesis, University of Buenos Aires, 1991.
- (50) Baraldi, I.; Carnevali, A.; Caselli, M.; Momicchioli, F.; Ponterini, G.; Berthier, G. *J. Mol. Structure: THEOCHEM*, **1995**, *330*, 403.
- (51) Michl, J.; Bonacic-Koutecky, V. *Electronic Aspects of Organic Photochemistry*; Wiley & Sons: New York, 1990.
- (52) Bonacic-Koutecky, V. *J. Am. Chem. Soc.* **1978**, *100*, 296.
- (53) Wong, M. W.; Frisch, M. J.; Wiberg, K. B. *J. Am. Chem. Soc.* **1990**, *113*, 4776.
- (54) Gegiou, D.; Muzkat, K. A.; Fischer, E. *J. Am. Chem. Soc.* **1968**, *90*, 12.
- (55) Sun, Y.; Saltiel, J. *J. Phys. Chem.* **1989**, *93*, 8310.
- (56) Bagchi, B.; Oxtoby, D. W. *J. Chem. Phys.* **1983**, *78*, 2735.
- (57) Levitus, M.; Negri, R. M.; Aramendía, P. F. *J. Phys. Chem.* **1995**, *99*, 14231.